Sensors and Actuators A 189 (2013) 177–181

Contents lists available at SciVerse ScienceDirect

Sensors and Actuators A: Physical

journal homepage: www.elsevier.com/locate/sna

A new compact micro-ball lens structure at the cleaved tip of microfiber coupler for displacement sensing

A.A. Jasim [a], A.Z. Zulkifli [a], M.Z. Muhammad [a], S.W. Harun [a,b,*], H. Ahmad [b]

[a] Department of Electrical Engineering, Faculty of Engineering, University of Malaya, 50603 Kuala Lumpur, Malaysia
[b] Photonics Research Center, Department of Physics, University of Malaya, 50603 Kuala Lumpur, Malaysia

ARTICLE INFO

Article history:
Received 28 May 2012
Received in revised form 4 September 2012
Accepted 4 September 2012
Available online 25 September 2012

Keywords:
Tapered fiber
Micro-ball lens
Displacement sensor

ABSTRACT

A compact micro-ball lens structure is fabricated at the cleaved tip of microfiber coupler (MFC) waist for displacement sensor application. The MFC is made by fusing and tapering two optical fibers using a flame brushing technique. It is then cleaved at the center of the minimum waist region. Then a micro-ball lens is formed at the tip of the microfiber by an arcing technique using a fusion splicing machine. The proposed displacement sensor uses the micro-ball lens as a probe and a reflector as a target. As the target is moved from the micro-ball lens, an interference fringe is obtained due to the interference between two reflected beams from the micro-ball lens and the reflector. At the smallest displacement of 0.6 mm, the output spectrum shows the interference fringes with highest extinction ratio and largest free spectral range (FSR). Both extinction ratio and FSR reduces following the power trend line with correlation coefficient of 0.99 as the displacement increases. The *Q* resonant factor of the comb spectrum increases from 1628 to 38,286 as the displacement increases from 0.6 to 3.6 mm.

1. Introduction

Microfibers with cross-sectional dimensions of the order of a few micrometers have received significant attention for applications in various areas such as lasing [1], sensing [2], filtering over wide spectral regions [3], and for nonlinear studies [4,5]. Furthermore, they can be manufactured via relatively simple top-down fabrication processes (such as flame [2] or laser-assisted tapering [6] and also micro-heater tapering [7]), wherein a standard heat-and-draw principle is employed. Recently, Fabry–Perot interferometers (FPIs) have extensively been explored in various sensing applications due to their high measurement sensitivities [8]. This interferometer is based on multiple-beam interference within two reflecting surfaces whereby the reflected light in the FPI is wavelength-modulated in exact accordance with the cavity length. Therefore it is suitable for various sensitive applications such as measuring velocity, displacement, strain, temperature and stiffness measurements [8–10].

Positioning technology is an important high precision technology useful for developing microsystems. In particular, displacement sensors are necessary for positioning devices with nano-scale accuracy. Much attention has also been focused on micro-ball lens in recent years for achieving low-cost coupling [11]. In earlier works [9,10], non-contact vibration measurement has been demonstrated using an external Fabry–Perot interferometer. In this paper, we propose a new displacement sensor using the same cavity formation but with a microfiber ball lens instead of a GRIN lens as a sensing probe. The probe is made at the minimum waist region of microfiber coupler (MFC), which is cleaved to form a micro-ball lens using an arcing technique. This sensor has a wide measuring range, high resolution, and excellent accessibility for narrow target areas. The proposed sensor uses both microfiber and microfiber ball lens, which is more compact compared to the conventional single mode fiber and multimode fiber.

2. Fabrication of the microfiber coupler and micro-ball lens

An MFC structure is made by laterally fusing and tapering two optical fibers using an experimental setup as shown in Fig. 1. In this experiment, a standard telecom optical fiber (Corning SMF-28) was used to make a low noise microfiber coupler with the aid of the well-known flame-brushing technique [2]. In the fabrication process, two fibers were brought into close proximity after their protective plastic jacket was removed. Then, both fibers were twisted at two different locations and heated by a torch to fuse and stretch them. The torch uses a mixer of butane and oxygen

* Corresponding author at: Department of Electrical Engineering, Faculty of Engineering, University of Malaya, 50603 Kuala Lumpur, Malaysia.
E-mail address: swharun@um.edu.my (S.W. Harun).

0924-4247/$ – see front matter © 2012 Elsevier B.V. All rights reserved.
http://dx.doi.org/10.1016/j.sna.2012.09.003

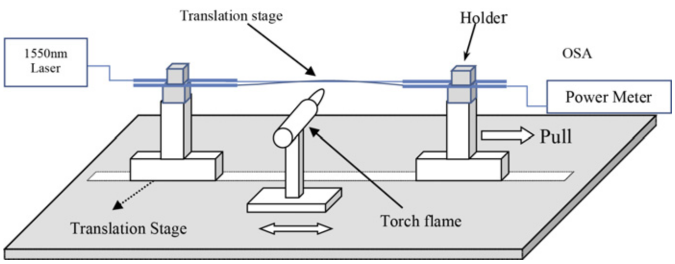

Fig. 1. Microfiber coupler fabrication setup.

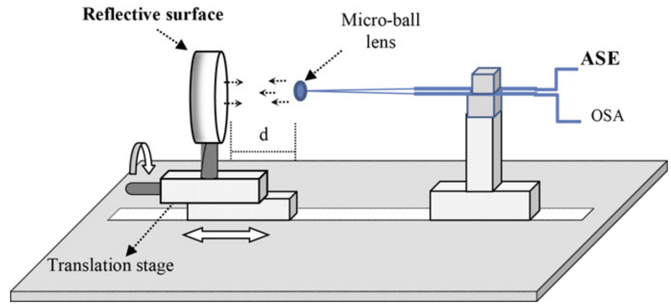

Fig. 3. The schematic diagram of the proposed displacement sensor.

gases to generate a flame with a temperature of around 1400 °C. The longitudinal profile of the conical transition taper was achieved by reliably controlling the heat infused into the hot zone and precisely moving the translation stages. During the tapering process, the coupling ratio was monitored in real time by using a 1550 nm light source and power meters. The heating and pulling processes were stopped the moment a 50/50 coupling ratio was achieved. The diameter of the MFC waist was about 5 μm and the lengths of tapered region and uniform waist were 70 mm and 40 mm, respectively.

The fabricated MFC was then used to form a micro-ball lens by an arcing technique using a fusion splicing machine. First, the MFC was cut at the center of the minimum waist region to form a micro-ball lens at the tip. The fabrication process involved two processes and they were loading and arcing processes. In the loading process, we opened the windshield of the splicer, the fiber holders and the fiber clamps and loaded the prepared MFC tip into the left side of the holder with the tapered region in the V-groove. It is important to make sure that the MFC is properly aligned in the V-groove before closing the fiber holder. The fiber clamp was closed afterwards to hold the fiber on the V-groove. Once the fiber was loaded correctly, the windshield was closed and finally the formation of the micro-ball lens started with the arching process. After setting the arc power, the cleaning arc power offset and the cleaning time, the fabrication of the micro-ball lens commenced. The MFC tip absorbed the arc discharging heat and melted instantaneously. Due to the surface tension, the melting part of the MFC started to form a spherical shaped tip gradually during solidification. As the spherical tip grew bigger, the effect of gravity increased and pulled the tip towards the ground. This causes the spherical tip to descend and increased the offset distance between the centre of the sphere and the axis of the fiber stylus. To avoid this misalignment, the MFC was rotated slowly while the tip solidified. Fig. 2(a) and (b) shows the microscope image of the micro-ball lens on the tip end of the MFC with and without the injection of red light, respectively. As shown in Fig. 2(b), the bright red color represents the scattering from the reflected red light.

Fig. 3 shows the experimental setup for the proposed micro-ball lens based displacement sensor with a reflective surface as a target. The reflector reflectivity at 1550 nm is estimated to be around 60%. The micro-ball lens coupler is fixed horizontally on a translation stage in front of a reflector at a distance (*d*). One of the coupler ports is connected to an amplified spontaneous emission (ASE) light source while the other port is connected to an optical spectrum analyzer (OSA) as shown in the figure. The reflector is held by another translation stage so that the displacement between the reflector and micro-ball lens can be varied.

3. Results and discussion

The schematic diagram of the probe and reflector is shown in Fig. 4, in which directions of the propagating light reflected inside the probe and outside the probe by the reflector are indicated. When the ASE light is injected into the micro-ball lens through the input port of the MFC, part of it is reflected by the micro-ball lens surface while some portion passes through the micro-ball lens and is reflected by the reflector. We denote I_1 as the part of light beam that is directly reflected by the inner surface of the micro-ball lens and I_2 as the portion that passes through the micro-ball lens and travels across the gap with a distance d before being reflected by the reflector. The reflected beams interfere in the micro-ball lens and in the medium as they travel to the output port of the coupler. The interference fringe is recorded at OSA as shown in Fig. 5. As the reflector is moved away from the sphere, the fringe weakens.

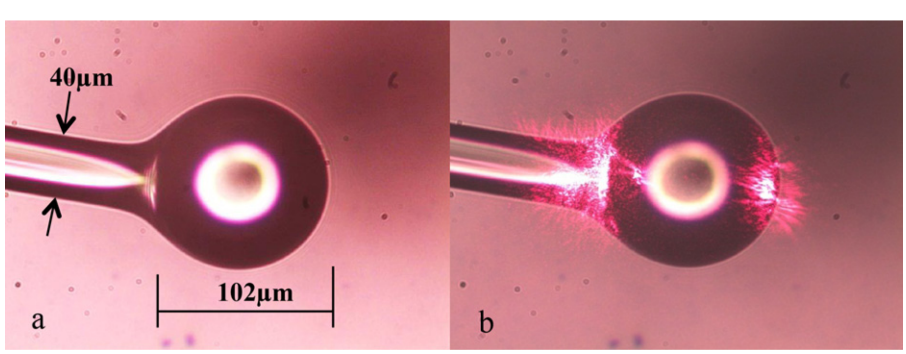

Fig. 2. Microscope images for the micro-ball lens fabricated at the cleaved tip of MFC (a) without injecting any light (b) with injection of red laser. (For interpretation of the references to color in the text, the reader is referred to the web version of the article.)

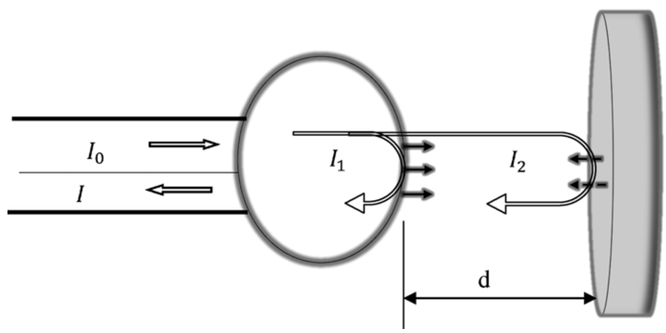

Fig. 4. Schematic diagram showing the light propagation inside the sensor probe and the reflector.

The interference spectrum can be modeled using the two-beam optical interference equation:

$$I = I_1 + I_2 + 2\sqrt{I_1 I_2}\cos(\Delta\phi) \quad (1)$$

where $\Delta\phi$ is the phase difference between two optical path length difference for the two beams of light, which is given by;

$$\Delta\phi = \left(4\pi \frac{n_d d}{\lambda} + \phi_o\right) \quad (2)$$

n_d and d are the refractive index of the air gap which is 1 and the gap displacement, respectively. Eq. (1) can be simplified as:

$$I = a + b\ \cos\Delta\phi \quad (3)$$

where a and b are arbitrary constants. The fringe spacing or free spectral range (FSR) is defined as the spacing between two adjacent minima or maxima in the reflection spectrum, which is given by the expression below [12]

$$\Delta\lambda = \frac{\lambda^2}{2d} \quad (4)$$

where λ is the operating wavelength. The contrast of the fringes is determined by

$$F = \frac{\text{FSR}}{\text{FWHM}} \quad (5)$$

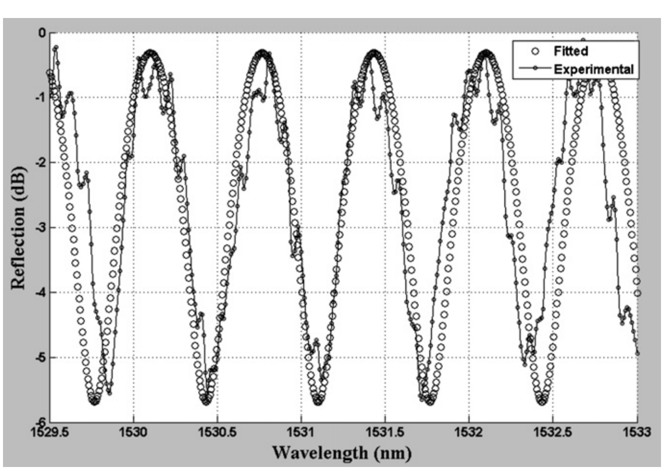

Fig. 5. The experimental data and its best-fit curve based on the values of d = 1.76 mm, a = 0.600 and b = 0.330.

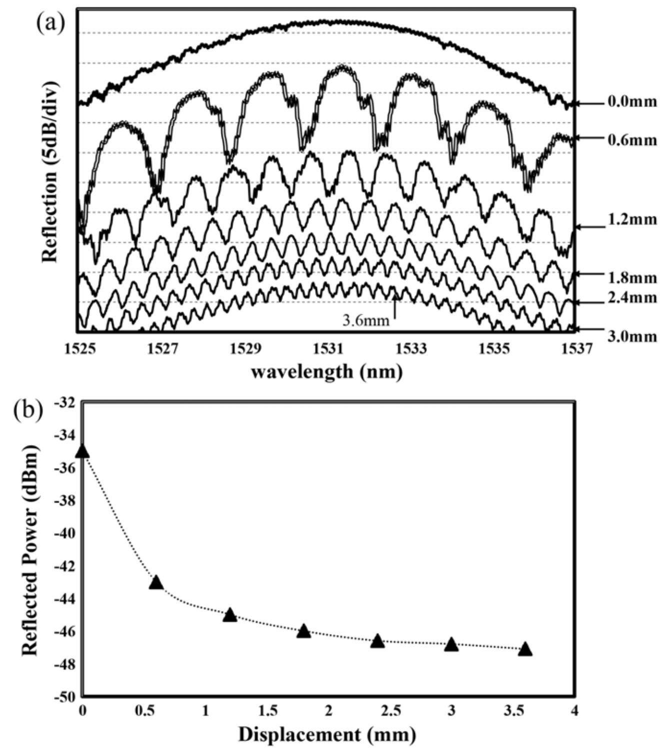

Fig. 6. Output spectra characteristics: (a) output spectra at various displacement of reflector from micro-ball lens and (b) reflected power against the displacement.

where F is the finesse of the cavity and FWHM is full-width half maximum of the spectrum. The relative displacement d of the target reflector surface is given by [8]

$$d = \frac{m\lambda}{2} \quad (6)$$

where m is the order of reflections. Fig. 5 shows the experimental data of the interference spectrum fitted with the theoretical model given by Eq. (3). The parameters for the best-fit curve are obtained as d = 1.76 mm, a = 0.600 and b = 0.330. The finesse of the cavity is calculated to be 2 at d = 1.76 mm. As also seen in Fig. 5, the measured interference pattern is not as smooth as the theoretical one, which is most probably due to the noise received from the higher order reflected beams.

Fig. 6(a) shows the output spectra recorded by the OSA against the displacement of the reflector. In the experiment, the displacement was varied by moving the reflector away from the micro-ball lens in a step of 0.6 mm. Initially, the micro-ball lens was positioned in contact with the reflector at d = 0. The output spectrum shows the highest output power but without any fringes. This indicates the absence of interference since I_1 and I_2 are nearly identical in phase since I_2 is immediately reflected by the reflector as the gap is zero. As the reflector is displaced by 0.6 mm, the output spectrum shows the interference fringes with the highest extinction ratio and largest fringes spacing. The interference fringes become weaker with smaller free spectral range (FSR) and extinction ratio as the gap increases. The relationship between the fringes spacing or FSR and the displacement can be explained by Eq. (4). The semicircle curves are due to the characteristics of the ASE light source used in this experiment. Fig. 6(b) shows the measured reflected optical power as a function of the displacement. As seen, the reflected power reduces from −35 dBm to −47.1 dBm as the displacement increases from 0 to 3.6 mm.

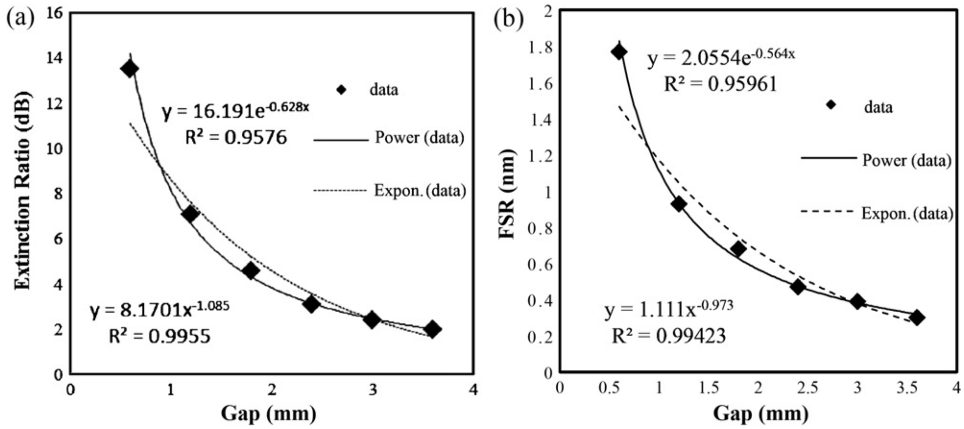

Fig. 7. (a) Extinction ratio and (b) FSR against the displacement.

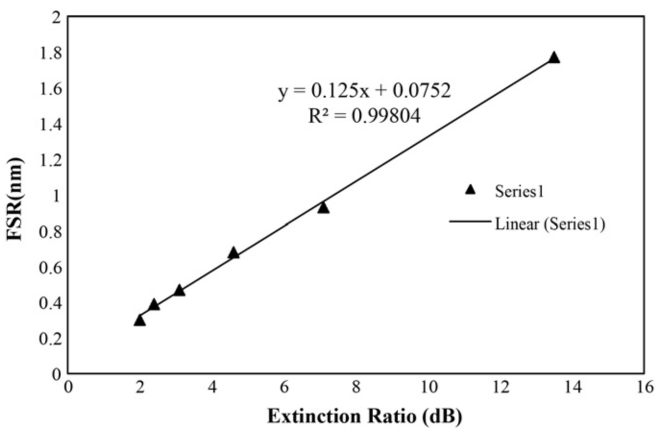

Fig. 8. Linear relationship between FSR and extinction ratio of the output comb of the sensor.

Fig. 7(a) and (b) shows the extinction ratio and FSR of the output comb as a function of displacement. Fitting curves of the experimental data are also presented in both figures using both power and exponential trend lines. It is found that the experimental data for both figures fits very well with both power and exponential trend lines with the correlation coefficient values of above 0.99 and 0.95, respectively. Fig. 8 shows a plot of FSR against extinction ratio, which displays a linear relationship with a correlation coefficient of more than 0.99. The *Q* resonant factor is also calculated from output spectra of Fig. 6. It is observed that the *Q*-factor increases from 1628 to 38,286 as the gap grows from 0.6 to 3.6 mm. The *Q*-factor is defined as the ratio of the wavelength resonance to the FWHM bandwidth of the interference fringes. The higher *Q* indicates a higher sensitivity of the displacement measurement. The cavity loss however, increases as the displacement increases, which in turn limits the measurement range of the sensor. At $d = 1.76$ mm, the finesse of the cavity is calculated to be 2, which is practical for sensing application.

4. Conclusion

A compact displacement sensor is demonstrated using a micro-ball lens structure fabricated at the cleaved tip of an MFC. The MFC is fabricated by fusing and tapering two optical fibers using a flame brushing technique while the micro-ball lens is formed at a cleaved tip of the MFC using an arcing technique. The micro-ball lens acts as a probe while a reflector acts as a target. There is no interference when the micro-ball lens is touching the reflector at the initial position. An interference fringe is observed as the target is moved away from the micro-ball lens due to the interference between two reflected beams from the micro-ball lens and the reflector. Both the extinction ratio and FSR of the comb spectrum reduces following the power trend line with correlation coefficient of 0.99 as the displacement increases. At the smallest displacement of 0.6 mm, the output spectrum shows the interference fringes with the highest extinction ratio and largest free spectral range (FSR). The *Q* resonant factor of the comb spectrum increases from 1628 to 38,286 as the displacement increases from 0.6 to 3.6 mm.

Acknowledgement

S.W. Harun would like to thank the University of Malaya for the financial support under the HIR Grant (no. D000009-16001).

References

[1] X. Jiang, Q. Song, L. Xu, J. Fu, L. Tong, Microfiber knot dye laser based on the evanescent-wave-coupled gain, Applied Physics Letters 90 (2007) 233501–233511.
[2] K.S. Lim, S.W. Harun, S.S.A. Damanhuri, A.A. Jasim, C.K. Tio, H. Ahmad, Current sensor based on microfiber knot resonator, Sensors and Actuators A: Physical 167 (1) (2011) 60–62.
[3] Y. Chen, Z. Ma, Q. Yang, L.-M. Tong, Compact optical short-pass filters based on microfibers, Optics Letters 33 (2008) 2565–2567.
[4] G. Vienne, L. Yuhang, L. Tong, P. Grelu, Observation of a nonlinear microfiber resonator, Optics Letters 33 (2008) 1500–1502.
[5] S. Leon-Saval, T. Birks, W. Wadsworth, P. St, J. Russell, M. Mason, Supercontinuum generation in submicron fibre waveguides, Optics Express 12 (2004) 2864–2869.
[6] A.J.C. Grellier, N.K. Zayer, C.N. Panell, Heat transfer modeling in CO laser processing of optical fibres, Optics Communication 152 (1998) 324–328.
[7] G. Brambilla, F. Koizumi, X. Feng, D.J. Richardson, Compound glass optical nanowires, Electronics Letters 41 (2007) 400–402.
[8] T. Steinmetz, Y. Colombe, D. Hunger, T.W. Hänsch, A. Balocchi, R.J. Warburton, J. Reichel, Stable fiber-based Fabry–Pérot cavity, Applied Physics Letters 89 (2006) 111110.
[9] T.K. Gangopadhyay, Non-contact vibration measurement based on an extrinsic Fabry–Perot interferometer implemented using arrays of single-mode fibres, Measurement Science And Technology 15 (2004) 911–917.
[10] T.K. Gangopadhyay, P.J. Henderson, Vibration: history and measurement using an extrinsic Fabry–Perot sensor with solid-state laser interferometry, Applied Optics 36 (1999) 2471–2477.
[11] H. Yang, C.K. Chao, C.P. Lin, S.C. Shen, Micro-ball lens array modeling and fabrication using thermal reflow in two polymer layers, Journal of Micromechanics and Microengineering 14 (2004) 277–282.
[12] J.C. Wyant, Introduction to interference and interferometry, part 5, University of Arizona, 2000, pp. 7–9.

Biographies

Ali Abdulhadi Jasim received his B.Sc. in Electrical Engineering from University of Technology, Baghdad, Iraq, in 2007 and M.Eng. degree in Telecommunication from University of Malaya, Malaysia, in 2010. He is currently pursuing his Ph.D. program at University of Malaya. His current field of interests is optical micro/nanofibers photonic devices with its applications.

Ahmad Zarif Zulkifli received his B.Eng. in Electrical & Electronics Engineering from University of Technology, Malaysia in 2008 and M.Eng. in Telecommunication Engineering from University of Malaya, Malaysia, in 2010. He is currently pursuing his Ph.D. program in optical fiber devices at Photonics Research Center, University of Malaya.

Mohd Zuhdin Muhammad received the B.E. degree in Electrical and Electronics Engineering from Saga University, Japan in 1997. Currently he is pursuing his Ph.D. program in University of Malaya, Malaysia.

Sulaiman Wadi Harun received the B.E. degree in Electrical and Electronics System Engineering from Nagaoka University of Technology, Japan in 1996, and M.Sc. and Ph.D. degrees in Photonics from University of Malaya in 2001 and 2004, respectively. Currently, he is a full professor at the Faculty of Engineering, University of Malaya. His research interests include fiber optic active and passive devices.

Harith Ahmad received the Ph.D. degree in laser technology from the University of Swansea (U.K.) in 1983. He is a full professor at the Department of Physics, University of Malaya. He is also a fellow member of Malaysian Academic of Science.